small NANO MICRO

Quantum Dots

Quantum-Dot-Encoded Microbeads for Multiplexed Genetic Detection of Non-amplified DNA Samples

*Yali Gao, William L. Stanford, and Warren C. W. Chan**

Barcoding technologies have become the basis for a new generation of molecular diagnostic platforms for measuring biomarkers in a high-throughput, rapid, and sensitive manner. Thus far, researchers have mainly focused on preparing different types of barcodes but, in order to use them optimally in genomic- and proteomic-based applications, there is a need to understand the effect of barcode and assay parameters on their performance. Herein, quantum-dot barcodes are systematically characterized for the detection of non-amplified DNA sequences. The effect of capture probes, reporter probes, and target DNA sequence lengths are studied, as well as the effect of the amount of noncomplementary sequences on the hybridization kinetics and efficiency. From DNA denaturation to signal detection, quantum-dot-barcode assays require less than one hour to detect a target DNA sequence with a linear dynamic range of 0.02–100 fmol. Three optically distinct quantum-dot barcodes are used to demonstrate the multiplexing capability of these barcodes for genomic detection. These results suggest that quantum-dot barcodes are an excellent platform for multiplex, rapid, and sensitive genetic detection.

1. Introduction

Significant efforts are being made towards the development of cost-effective, sensitive, and selective diagnostic devices capable of screening a wide variety of diseases. Enzyme-linked immunosorbent assays (ELISA) and lateral-flow immunoassays (LFI) for protein detection and polymerase chain reaction (PCR) for DNA detection are currently the gold standards in molecular diagnostics. Microbeads are a promising and versatile diagnostic platform but have not been fully developed. In a typical microbead assay, antibodies, peptides, oligonucleotides, or other targeting agents are conjugated onto the microbead surface. This bead complex captures complementary molecules of interest in buffer or clinical fluids, such as plasma, serum, or urine. Next, the beads are washed and incubated with a fluorescently labeled secondary targeting agent. Detection occurs when the fluorescence of the beads is measured with a flow cytometer[1] or a microfluidic system.[2] The advantages of microbeads for diagnostics include: 1) the inexpensive production of microbeads, 2) the capability of detecting either proteins or genes, 3) faster reaction kinetics, 4) well-established bead synthesis protocols, and 5) the tunability of bead size. Microbeads can be encoded with optical emitters such as quantum dots (QDs),[3,4] organic fluorophores,[1,5] and raman probes[6] for multiplex analysis of biological targets. Beads could also be engineered to detect molecules in biological fluids,[7,8] inside cells,[9,10] and as probes for in vivo imaging applications.[11,12] Despite these advantages, microbead assays have found limited use in clinical and research settings, as compared to ELISA, LFI, PCR, and other molecular techniques.

Microbead barcodes doped with organic fluorophores were first introduced in the 1990s and are currently commercially available for molecular detection. However, organic fluorophores have numerous limitations for coding

Dr. Y. Gao, Prof. W. L. Stanford, Prof. W. C. W. Chan
Institute of Biomaterials & Biomedical Engineering
University of Toronto
Toronto, ON, M5S 3G9, Canada
E-mail: warren.chan@utoronto.ca
Prof. W. C. W. Chan
Donnelly Center for Cellular and Biomolecular Research
Departments of Materials Science and Engineering
Chemistry, and Chemical Engineering
University of Toronto
Toronto, ON, M5S 3G9, Canada

DOI: 10.1002/smll.201000909

microbeads, such as the requirement of multiple laser-excitation sources, a broad fluorescence spectrum that limits the number of available barcodes, photobleaching that can affect the accuracy of detection, and the leaking of fluorophores from the barcode matrix. These challenges have promoted the use of alternative optical fluorophores such as QDs for doping microbeads to create barcodes.[3,13] The advantages of QDs for coding include: a tunable emission wavelength, a narrower fluorescence spectra than organic fluorophores, and a broad excitation wavelength (enabling the excitation of multiple colors by a single-wavelength source). Therefore, the use of QDs for coding would lead to a larger number of barcodes than organic fluorophores and would simplify the design and cost of the read-out device. There is great potential for QD-encoded microbeads, that is, quantum dot-barcodes (QdotBs), to become the next generation of barcodes. However, a number of challenges remain to make them a commercially viable technology. These challenges include the development of deconvolution algorithms to identify the beads,[14] the preservation of the fluorescence inside the beads, the optimization of chemistry to conjugate targeting agents onto the bead surface, the simplification of the bead assay, and the suppression of nonspecific binding. Our lab has been interested in addressing these problems to create a QdotBs platform for infectious-disease detection. We have developed new strategies to prepare QdotBs,[15] characterized their surface chemistry,[16] evaluated methods to deconvolve the optical signal,[17] and developed a microfluidic platform to read out their signal[18] for the purpose of developing a handheld diagnostic device for use in the developing and developed world.

Surprisingly, there have been limited studies on the use of QdotBs for multiplex genetic analysis. Xu et al. have used QD-encoded beads for genotyping ten single-nucleotide polymorphisms of PCR-amplified genomic DNA.[19] Eastman et al. employed magnetic microbeads encoded with four colors and twelve intensity levels of QDs for gene-expression analysis with comparable accuracy and sensitivity to microarray.[20] In spite of the demonstrated promising applications, there is a lack of fundamental studies on optimizing the barcode assay's performance in detecting biological samples. Moreover, in these experiments, tedious and slow procedures were required for the pretreatment of biological samples, such as the isolation and purification of the genetic material (e.g., DNA) followed by PCR and electrophoresis analysis prior to barcode assays.

Here, we characterized a QdotB-based genetic assay using restriction-digested plasmid DNA fragments without an amplification step. DNA was initially purified and the target was obtained simply by digestion with one or several restriction enzymes at 37 °C. We studied the effect of capture probes, reporter probes, and target-DNA sequence lengths as well as the amount of noncomplementary sequences on the hybridization kinetics and efficiency. Without isolation and purification, we demonstrated that multiple genes could be detected simultaneously with different QdotBs. These results have implications in the design of an automated self-contained QdotB assay system for genetic diagnostic testing.

Table 1. A list of the plasmid DNA used.

Plasmid	Size [kb]	Genes
pSD5	7.8	*Amp, Neo, Lac Z*
pCX-ECFP	5.5	*Amp*
pBS64	3.1	*Amp*
plox511pneo	4.8	*Amp, Neo*
pPGK-neo-FRT	4.8	*Amp, Neo*
pHTR3-B	10.0	*Amp, Neo, Lac Z*
pGTlox4	9.1	*Amp, Lac Z*
pDONR211	4.8	-

2. Experimental Details

2.1. Isolation and Digestion of Plasmid DNA and Design of Probes

Host bacteria cells, *Escherichia coli* DH5α, encoding different plasmid DNA, were inoculated into lysogeny broth (LB) medium (200 mL for Maxiprep, or 5 mL for Miniprep) with ampicillin (75 μg mL^{-1}). The bacteria cells were grown overnight at 37 °C and 250 rpm in an orbital shaker. The main positive-control plasmid pSD5[21] and the main negative-control plasmid pCX-ECFP[22] were purified using NucleoBond Xtra Maxi Columns (Clontech Laboratories, Inc. Mountain View, CA). Plasmid DNA used in the multiplex hybridization assay, including pBS64,[23] plox511pneo,[24] pPGK-neo-FRT,[24] pHTR3-B,[24] and pGTlox4,[21] were purified using GeneJet Plasmid Miniprep Kit (Fermentas Inc, Glen Burnie, MD), according to the manufacturer's instructions. The purified DNA's concentration was measured via UV absorption at 260 nm by using a Nanodrop spectrophotometer ND-1000 (Nanodrop technologies, Wilmington, DE). A negative-control plasmid pDONR211was obtained from Invitrogen (Carlsbad, CA). **Table 1** shows a list of the sizes of the different plasmid DNA, as well as the relevant genes they carry.

Restriction digestion of plasmid DNA was designed with RestrictionMapper v3.0 (http://www.restrictionmapper.org/). The sequences for target-fragment and corresponding-probe sets are shown in **Table 2**. In the assays for *Neomycin* (*Neo*) in pSD5, the three target fragments of 36, 81, and 197 bp were obtained by digesting pSD5 with restriction enzymes *Eae*I, *Bbv*I, and *Pst*I, respectively. For the multiplex hybridization assay, three enzymes, *Eae*I, *Hph*I, and *Hga*I, were used together to generate the 36-bp target fragment for *Neo*, as well as a 37-bp target fragment for *Lac Z* and a 46-bp target fragment for *Ampicillin (Amp)*. All restriction enzymes were purchased from New England Biolabs (Ipswich, MA) and restriction digestion was conducted according to the manufacturer's instructions. After digestion, agarose gel electrophoresis (1% agarose) was performed to check that the digested fragment patterns were as designed. Digested DNA was kept at 4 °C until use. The oligonucleotide probes were synthesized by Integrated DNA Technologies (Coralville, IA). The capture probes were modified with an amino group at the

small NANO MICRO

Table 2. Sequence for the target fragments and probe sets.

Gene	Size [bp]	Sequence (5′→ 3′)[a]
Neo	36	GGCCGGAGAACCTGCGTGCAATCCATCTTGTTCAAT
	81	TGTTGTGCCCAGTCATAGCCGAATAGCCTCTCCACC-CAAGC**GGCCGGAGAACCTGCGTGCAATCCATCTT-GTTCAAT**GGCC[b]
	197	GTTCATTCAGGGCACCGGACAGGTCGGTCTT-GACAAAAAGAACCGGGCGCCCCTGCGCTG-ACAGCCGGAACACGGCGGCATCAGAGCAG-CCGATTGTCTGTTGTGCCCAGTCATAGCCGAA-TAGCCTCTCCACCCAAGC**GGCCGGAGAACCT-GCGTGCAATCCATCTTGTTCAAT**GGCCGATCC-CATATTGGCTGCA[b,c]
LacZ	37	GTCACACTGAGGTTTTCCGCCAGACGCCACTGCTGCC
Amp	46	ACCAAGTCATTCTGAGAATAGTGTATGCGGCGAC-CGAGTTGCTCTT

[a]The two underlined regions for each target strand correspond to the reporter probe and the capture probe respectively. All capture probes are modified at the 5′ end with the amino group, as well as C12 and 9dTs as the spacer. The reporter probes are modified with Alexa Fluor 647 at the 3′ end. For example, for the 36-bp target of *Neo*, the capture probe is 5′-aminoC12-TTTTTTTTT-ATTGAACAAGATGGATTG. The reporter probe is GCAGGTTCTCCGGCC-Alexa647–3′. The three capture probes for *Neo* are 18-, 45-, and 91-nucleotides (nt) long, respectively. The three reporter probes for *Neo* are 15-, 33-, and 97-nt long, respectively. [b]The sequence of the 36-bp target strand is part of the 81-bp target strand, which is part of the 197-bp target strand. For clarity, the sequence of the 36-bp target is set in bold in the 81-bp and 197-bp target sequences. [c]For the 197-bp target of *Neo*, Alexa647 is conjugated at the 5′ end of the reporter probe, due to the technical difficulties of conjugating the dye at the 3′ end of an oligonucleotide at this size.

5′ end to bond with the carboxyl group on the microbeads. C12 and 9(dT) were added as a spacer between the amino group and the capture probe sequence. The reporter probes were conjugated with Alexa Fluor 647 for signal detection.

2.2. Conjugation of Capture Probe to QdotB

The QdotBs were polystyrene microbeads with an average diameter of 5 μm. Blank microbeads, without embedded QDs, were used in single-plex assays for the gene of *Neo,* for the optimization of assay conditions. For the multiplex assays of three different genes, the QdotBs were doped with different ratios of ZnS-capped CdSe QDs emitting at 500 and 600 nm, respectively, using a continuous-flow focusing approach.[15] We adapted a previously described procedure to coat the QdotBs with genetic-targeting agents.[16] Briefly, 5×10^6 of water-suspended QdotBs were pelleted and resuspended with 2-(*N*-morpholino)ethanesulfonic acid (MES buffer, pH 4.5, 350 μL). *N*-(3-Dimethylaminopropyl)-*N*′-ethylcarbodiimide hydrochloride (EDC, Sigma-Aldrich) (50 mg) was dissolved in MES buffer (pH 4.5, 150 μL) and added to the QdotB suspension. Finally, a capture probe (82 pmol, unless specified otherwise) was added and vortex-mixed with the QdotB suspension. The mixture, in a microcentrifuge tube, was incubated overnight on a rotator. The next day, MEST (MES buffer, 0.1% Tween, pH 4.5, 300 μL) was added to the QdotB mixture to wash the beads. After incubation at room temperature for 5 min, the QdotBs were pelleted and resuspended with PBST (phosphate buffered saline 1×, pH 7.4, 0.1% Tween, 200 μL), then kept at 4 °C and used within 24 h.

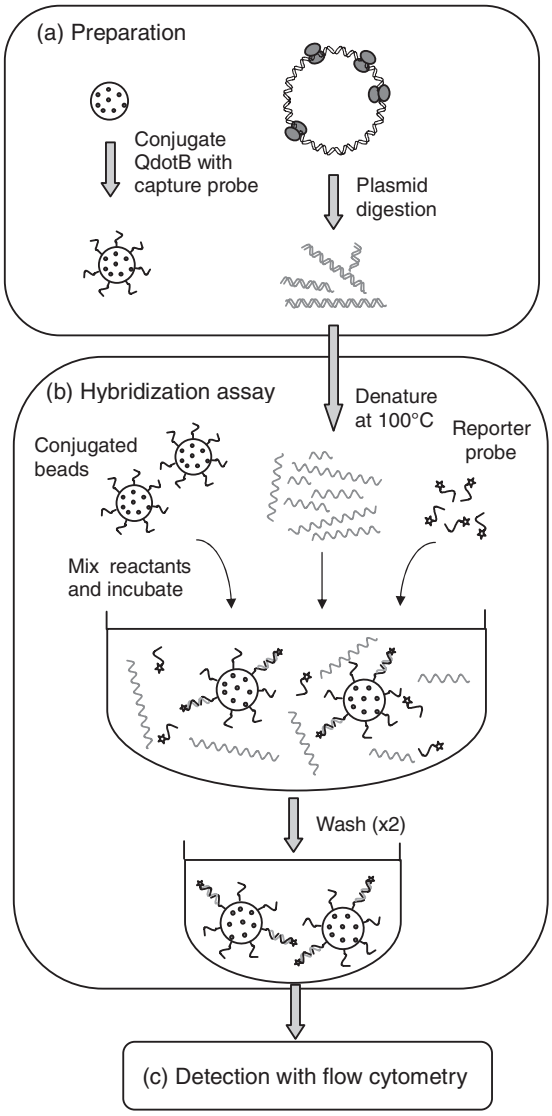

Figure 1. Schematic of the hybridization assay for digested plasmid DNA. a) QdotBs were conjugated with capture probe molecules using carbodiimide chemistry. Plasmid DNA was digested by a restriction enzyme into fragments. b) Right before the hybridization assay, digested DNA was denatured into single-stranded fragments. The denatured DNA was mixed with conjugated beads and the reporter probe, allowed to hybridize at room temperature, and washed twice. c) The fluorescent signal on the QdotB was detected using flow cytometry.

2.3. QdotB-Based Sandwich Hybridization of Digested DNA

A schematic of the sandwich-hybridization assay is shown in **Figure 1**. The digested double-stranded DNA was diluted to the desired concentration and denatured by heating at 100 °C for 5 min. Afterwards, the microcentrifuge tubes containing denatured DNA solution were taken off the heat block and immediately cooled on ice for 2 min. 6 μL of this sample DNA solution was then added to the reaction mixture containing 10 μL of hybridization buffer, i.e., 10× saline-sodium

citrate (SSC), 0.1% sodium dodecyl sulfate (SDS), 2 mM ethylenediaminetetraacetic acid (EDTA), pH 7.0. 2 μL of PBST-suspended QdotB suspension (containing ≈50 K beads conjugated with 0.82 pmol of capture probe, unless otherwise specified), as well as 2 μL of reporter-probe solution (containing 4 pmol of reporter probe, unless otherwise specified). For multiplex assays, different QdotB suspensions (each conjugated with different capture probes) and different reporter-probe solutions were mixed together. The reaction mixture was then vortex mixed and incubated on a rotator for 30 min or as specified. After hybridization, washing was performed by adding washing buffer (0.5 × SSC, 0.1% SDS, 200 μL) to the reaction mixture. The whole solution was then transferred to a 96-well screen plate with 0.45-μm-sized pores at the bottom membrane (Millipore, Billerica, MA). The solution was expelled by applying a vacuum from the bottom of the plate with the aid of a plate holder. The QdotBs left in each well were subjected to another washing cycle and then resuspended in PBST (200 μL) for flow-cytometry detection.

In the kinetics study (mainly in Section 3.2), according to the time points for measurement, the amount of each reagent was proportionally larger. For example, if there were five time points to be measured at (5, 10, 20, 30, and 45 min), the hybridization mixture was composed of 30 μL of sample DNA, 50 μL of buffer, 10 μL of PBST-suspended QdotB (conjugated with capture probe) suspension, and 10 μL of reporter probe. Then, at each time point, an aliquot of 20 μL was extracted from the hybridization mixture and subjected to washing, following the same washing protocol as described above.

2.4. Signal Detection with Flow Cytometry

The QdotBs were detected using BD FACSCalibur flow cytometer and associated CellQuest Software (Becton Dickinson, San Jose, CA). The collected data were analyzed using the software of FlowJo (Ashland, OR). For each hybridization assay, approximately 1500–2500 (single-plex) or 5000–6000 (multiplex) of size-gated QdotBs were used for signal analysis. For multiplex assays, identification of the QdotBs was done by mapping the fluorescence profiles from FL1 (530/30) and FL2 (585/42).

3. Results and Discussion

3.1. Defining QdotB-Based Hybridization

The basic reaction scheme $Cp + T + Rp \rightarrow C_h$ can be used to describe the QdotB's sandwich hybridization process. *Cp* stands for the capture probe immobilized on QdotB, *T* for the target DNA, *Rp* for the reporter probe, and C_h for the hybridization product of the *Cp*:*D*:*Rp* conjugate. The product yield can be improved by increasing the concentration of capture probe and reporter probe, as well as the rate constant k_h. These parameters were characterized in the study to optimize the assay.

3.1.1. Effect of Capture Probe Concentration

The amount of capture probe can be optimized by varying either the number of QdotBs per assay or the number of molecules immobilized on each QdotB. Increasing the number of beads will enhance the overall hybridization efficiency and precision of the assay; however, it will reduce the average number of target molecules bound per bead and the corresponding detection signal from flow-cytometry measurement. It was found that 50 000 beads per assay provided a good compromise between signal intensity and precision of measurement. Hybridization assays were then conducted against the amount of loaded capture probe. Three different sizes of capture probes were tested, each hybridized to a different size of DNA target for the gene of *Neo*, as shown in Table 2. As illustrated in **Figure 2**a, hybridization to the shortest probe of 18 nt demonstrated the strongest dependence on the amount of capture probe. While a low surface density of 0.03 molecules nm^{-2} (assuming all loaded capture probe was attached to the bead surface) did not provide enough sites to saturate the surface, a density as high as 0.25 molecules nm^{-2} apparently impaired the hybridization efficiency. The inhibited hybridization was likely due to steric crowding as well as repulsive electrostatic forces at high surface probe density. The optimal surface density of 0.13 molecules nm^{-2} is in agreement with earlier findings of 0.067 molecules nm^{-2} with DNA hybridization on polystyrene beads[25] and higher than those found with gold surface (0.02–0.06 molecules nm^{-2}),[26,27] probably due to the greater surface roughness of polymer beads.[16]

For the 45- and 91-nt probes, there was less dependence on the amount of loaded capture probe in the assay as compared to the smaller probe. This is perhaps because longer probes (longer than 24 nt, according to the study of Steels et al.[28]) do not stick rod-like to the surface like short ones but tend to form a coil-like secondary structure with much larger footprints, that is, surface area occupied by the immobilized probe ($R_g = 0.38N^{1/2}$ nm; R_g stands for the radius of gyration and *N* for the number of nucleotides in the probe[29]). Therefore, at high loading amount, the layer of long oligonucleotides would be less densely packed compared to short oligonucleotides and thereby relieving the steric effects during hybridization. The loading amount of 1×10^7 DNA $bead^{-1}$ was chosen as the optimal condition for all three of the capture probes. This equates to 0.83 pmol of capture probe per assay for 50 000 beads.

3.1.2. Effect of Reporter-Probe Concentration

Conventionally, a minimum of 1–2 orders of excess reporter probes in comparison to sample DNA is required to expedite a hybridization reaction.[30,31] The optimization of the amount of reporter probe in our assay system is illustrated in Figure 2b. The error bars represent the standard deviation of three duplicates. For both levels of target DNA tested (10 fmol and 1 fmol), hybridization efficiency increased with the amount of reporter probe with a similar trend. There was nearly a linear increase from 4 to 400 fmol that gradually reached a saturation point. In the presence of higher doses of reporter probe (>4 pmol), the amount of capture probe

small

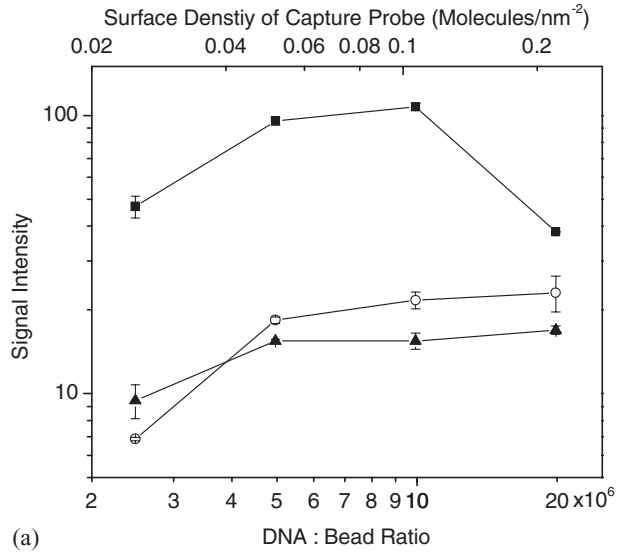

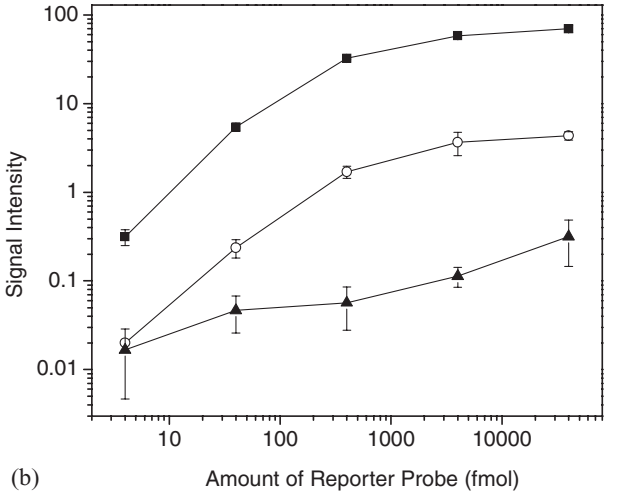

Figure 2. Effect of the loading amount of a) capture probe b) and reporter probe on hybridization. In (a), the three curves correspond to the hybridization of capture probes of 18 nt (-■-), 45 nt (-○-) and 91 nt (-▲-) to target DNA fragments of 36, 81, and 197 bp and reporter probes of 15, 35, and 97 nt, respectively, as in Table 2. The amount of target DNA and reporter probe was 10 fmol and 4 pmol, respectively. The top *x*-axis was the calculated surface density of capture probe, assuming all loaded capture probe was attached to the bead surface. In (b), the three curves are all from the hybridization of the 36-bp target to its capture probe (18 nt) and reporter probe (15 nt) and each curve corresponds to a target DNA amount of 10 fmol (-■-), 1 fmol (-○-), or negative control (no DNA) (-▲-), respectively. Error bars represent the standard deviation from three duplicate experiments.

(0.83 pmol) became the major restriction factor for hybridization. Also, the increase of the amount of reporter probe resulted in elevated levels of background signal from negative control. From the results, the amount of reporter probe for the study was chosen to be 4 pmol, for optimal signal/noise ratio and a wide dynamic range of the assay.

3.1.3. Effect of Salt Concentration

The hybridization rate constant is predominantly dependent upon salt concentration and hybridization temperature.

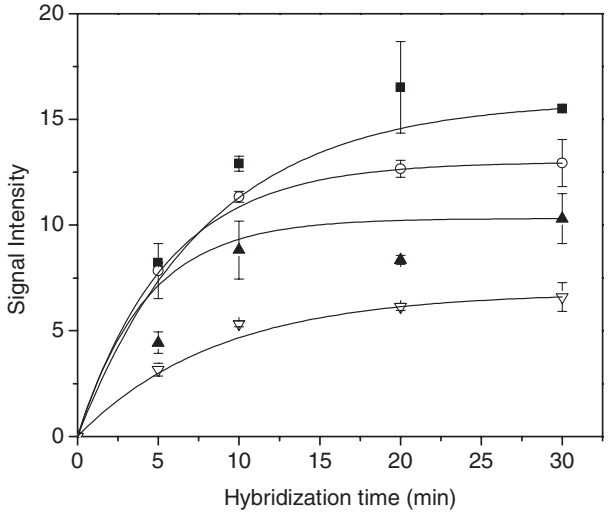

Figure 3. Effect of salt concentration on hybridization. The four curves are all from the hybridization of the 81-bp target to its capture probe (45 nt) and reporter probe (33 nt). Each curve corresponds to the hybridization buffer of 10 × SSC (-■-), 5 × SSC (-○-), 2 × SSC (-▲-), and 1 × SSC (-▽-), respectively, with 0.05% SDS and 1 mM EDTA. The salt concentration here was the final concentration in the hybridization mixture. For example, for the condition of 10 × SSC, the hybridization solution contained 10 μL of 20 × SSC, and 10 μL of reactants diluted in water or low-concentration buffers. The error bars represent the standard deviation of three duplicates.

To simplify the hybridization protocol, we avoided heating and conducted all the experiments at room temperature. The kinetic data shown in **Figure 3** was fit with the equation $C = C_0(1-e^{-kt})$, where C is the signal intensity, C_0 is the signal intensity at equilibrium, k is the rate constant, and t is the time. Salt concentration did not affect the reaction kinetics but improved the hybridization efficiency. Though 10 × SSC would be most favorable in terms of hybridization yield, such a high salt concentration was found to impair the stability of QdotBs and caused the beads to swell and break upon prolonged incubation (>1 h). Therefore, 5 × SSC was chosen as the optimal condition. 1 mM of EDTA was added to the hybridization buffer to enhance the stability of the polymer beads in the high-salt environment.

3.2. Optimization of the Hybridization Assay for Digested Plasmid

Unlike most studies on genetic detection, this study used digested plasmid rather than PCR amplicons as the assay target. Restriction enzymes can cut the plasmid and the targeted gene into variable fragment sizes. It is essential to understand how to design digestion and probes for optimal hybridization performance. Therefore, we varied the target fragment and probe size and studied their effect on hybridization.

The first parameter investigated was the target size. While fixing the capture probe and reporter probe at 18 and 15 nt, respectively, we tested three different target sizes, 36, 81, and 197 bp. The probe set (capture probe and reporter probe) was

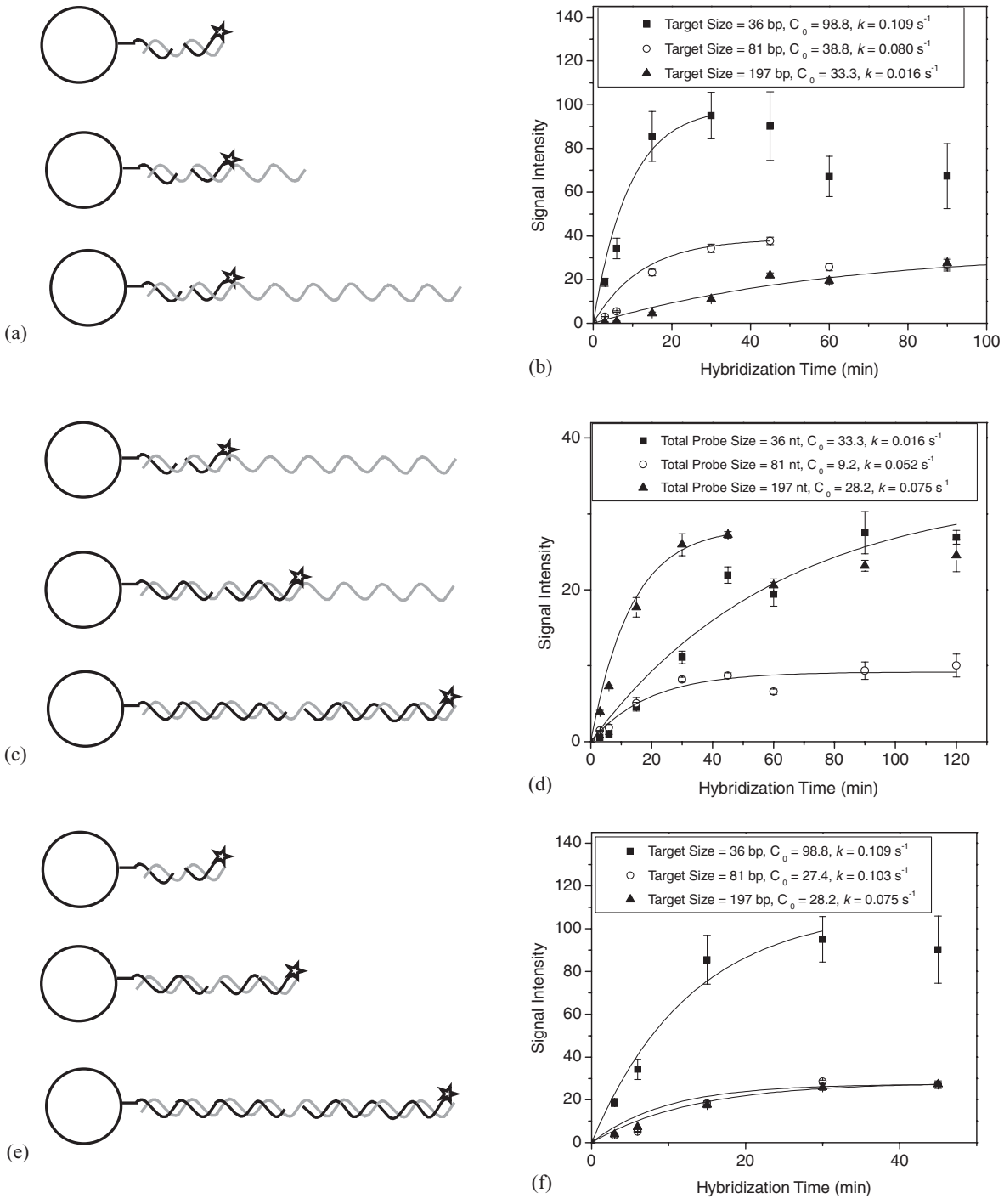

Figure 4. Dependence of hybridization kinetics on plasmid digestion and probe design: a,c,e) schematic of the assay design; b,d,f) corresponding assay results. Panels a and b show the effect of target size on hybridization, where the size of the probes was fixed at L_{cp} = 18 nt, L_{rp} = 15 nt. Panels c and d show the effect of the size of probe sets on hybridization, with L_{target} = 197 bp. Panels e and f show the effect of the target size on hybridization when the size of the probes were also varied to cover the full length of the target. The third curve (-▲-) in b and the first curve (-■-) in d are from the same data. Also, the first and third curves in f share the same data with the first curve in b and the third curve in d, respectively. The error bars represent standard deviations from three duplicate experiments. Of note, a decrease in the signal intensity for 36-bp target size in b was due to the degradation of microbeads after 30 min.

designed to sandwich hybridize to the full length of the 36-bp fragment, only leaving a 3-nt gap in between. The 81-bp and 197-bp target also shared common targeted sequence with the 36-bp target, as shown in bold letters in Table 2. A schematic of the hybridization assay is illustrated in **Figure 4**a. Figure 4b shows the kinetic data fit with the equation $C = C_0(1-e^{-kt})$. The smallest target (36 bp) was the optimal target size with a hybridization half-life of 7.1 min. An increase in target length led to a significant decrease in both hybridization rate and efficiency. This drop can be associated with intramolecular

small NANO MICRO

base pairing for long targets,[32] which may hide the targeted sequence and slow the hybridization process. Also, the hybridization of large DNA molecules to the surface may also hinder the accessibility of neighboring capture probes and reduce the hybridization efficiency. This result is in agreement with the findings of Liu et al. with microarrays where DNA or RNA molecules from 10 s to over 1000 nucleotides long were hybridized to 18-mer probes and shorter targets were found to confer higher hybridization efficiency.[33] The error bars in Figure 4 stand for the standard deviation of three duplicates and shows the variability from one assay experiment to the next.

Next, we studied the hybridization of the 197-bp target with different probe lengths. The three probe sets were those designed for the full length of the 36-bp, 81-bp and 197-bp target for *Neo*, as shown in Table 2. Figure 4c,d shows a schematic of the assay and the results, respectively. The longer probe set with a total span of 197-nt did expedite the hybridization compared to the shortest 36-nt probe set. Though hybridization reached a comparable efficiency at equilibrium, the half-life was shortened by almost 4 times (42.6 min vs. 10.6 min) with the 197-nt probe set. We suspect that a longer probe has a greater probability of nucleation. As observed from solution hybridization, the rate constant k is proportional to the length of base-pairing sequence L when $L < 100$ and proportional to $L^{1/2}$ when $L > 100$.[34] In the solid-phase hybridization with microarray or microbeads, longer probes with an optimal size of 50–70 nt have an additional advantage of extending further into the solution to conquer the near-surface steric interference to hybridization.[35] While short oligonucleotide probes (20–25-nt long) provide the best specificity,[36] longer probes, with the same size to the target DNA in our case, can led to faster reaction kinetics in solid-phase hybridization and usually higher hybridization efficiency.[30,37–39] However, Figure 4d shows that the intermediate 81-nt probe set yielded the lowest hybridization efficiency. The low signal is believed to be associated not with the size of the probe but with the tendency of this specific 45-nt capture probe sequence to form extensive hairpin loops. It is important to note that, aside from the size, there exist other important considerations in probe design including the probe's secondary structure, ratio and positioning of GC/AT, melting temperature, and the potential to self-hybridize.[40] Probes with the same size can yield significantly different hybridization rates and efficiencies because of these factors.[33,41]

As hybridization to a target DNA strand appeared strongest when probes hybridized to its full length, we again compared the hybridization of the three different sizes of DNA target under this optimal condition for each (Figure 4e). From the results in Figure 4f, hybridization still favored the shortest target strand of 36 bp, whose hybridization efficiency was about 3.5 times higher than that of the two longer targets. The reason should lie in the larger footprint of the long capture probe, as discussed for Figure 2a, as well as the secondary structure of the target molecule itself.

In conclusion, the target DNA strand should be a short fragment with a size of about 35–50 bp for hybridization assays after digestion. The capture and reporter probes should be designed to hybridize to the full length of the target to provide the best sensitivity and specificity. Special care should also be taken to minimize intramolecular hairpin loops within target and probe strands. Hybridization of digested DNA is superior to that of PCR amplicons in terms of the flexible target size as PCR amplicons are usually hundreds to over a thousand nucleotides long.

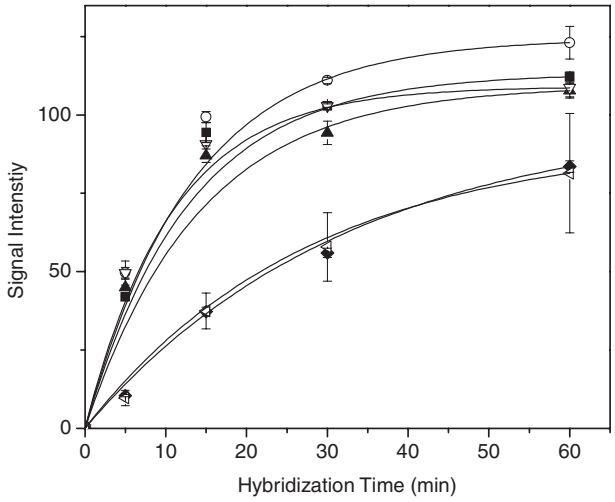

Figure 5. Effect of restriction digestion (fragment map) of pSD5 on hybridization. Each of the six curves corresponds to digestion with the enzymes (and average size of digested fragments) of: *Eae*I (-■-, 487 bp), *Eae*I + *Hph*I (-○-, 278 bp), *Eae*I + *Hae*II (-▲-, 251 bp), *Eae*I + *Hph*I + *Hae*II (-▽-, 169 bp), *Eae*I + *Bbv*I (-♦-, 152 bp), *Eae*I + *Bbv*I + *Hph*I (-◁-, 119 bp), respectively. The amount of sample DNA was 10 fmol for each assay.

Aside from the target DNA fragment, the digested plasmid also contained a large pool of noncomplementary differently sized DNA strands. We investigated whether noncomplementary strands in the reaction solution interfered with the hybridization process. This was accomplished by digesting the plasmid with several different enzymes and keeping the target fragment intact. As shown in **Figure 5**, hybridization was essentially independent of the average size of noncomplementary fragments. However, a drop in hybridization rate occurred whenever *Bbv*I was employed in digestion. The digestion of pSD5 by *Bbv*I yielded a small 3-bp fragment that hybridized to the capture probe and this fragment likely interfered with the designed hybridization. In practical applications, this matrix effect could be resolved by adding blocking reagents to the hybridization solution such as salmon sperm DNA.[38]

3.3. Dose–Response Curve

We then tested the dose–response curve of the QdotB-based hybridization assay with the optimal 36-bp target DNA strand and its corresponding probes. The hybridization time was 30 min. As shown in **Figure 6**, the assay had a wide dynamic range of 3.5 logs, from 0.02 fmol to 100 fmol. The lower limit of detection of 0.02 fmol (or 1 pM) was comparable or better than those from other microbeads-based hybridization

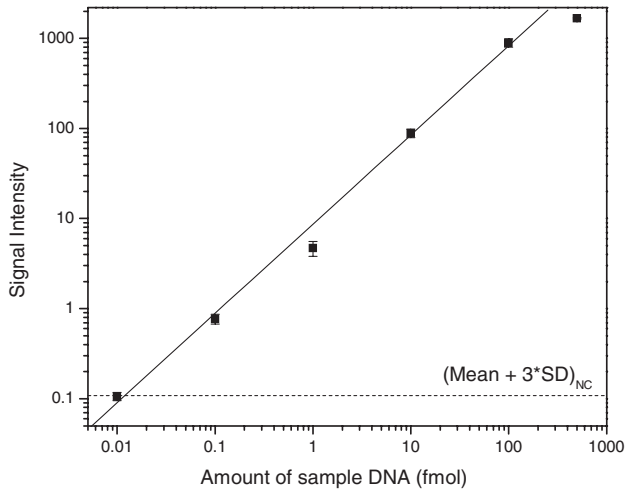

Figure 6. Dose-response curve of the hybridization assay. A linear fit was obtained with data points below 100 fmol. The size of the target strand, capture probe, and reporter probe are 36 bp, 18 nt, and 15 nt, respectively.

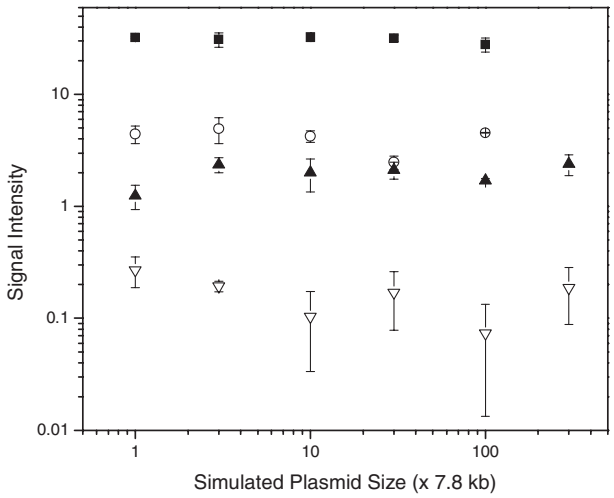

Figure 7. Hybridization with varying size of target DNA. Different-sized target DNA was simulated by spiking the negative-control plasmid (without *Neo*), pCX-ECFP, into the plasmid of pSD5. The data points correspond to sample DNA (pSD5) amount of 3 (-■-), 1 (-○-), 0.3 (-▲-), and 0.1 fmol (-▽-), respectively.

assays,[30,38,42–44] which are in the range of 0.03 fmol to 1 pmol. This is remarkable because other studies used synthetic oligonucleotides or PCR amplicons as a model analyte while the sample DNA being used here is much more crude, i.e., digested DNA with the presence of the target strand's original complementary strand, as well as a pool of nonspecific sequences. This demonstrates that unpurified genetic targets can be detected using QdotBs.

For the aimed future application of genetic diagnostics, the target molecule would be bacterial or viral genomic DNA, which can be several million base pairs in size, and there would be more nonspecific sequences in the sample solution. To examine whether nonspecific sequences interfere with the performance of the hybridization assay, we spiked various excessive amount of nonspecific sequences (from the plasmid of pCX-ECFP) into the sample DNA solution, to simulate differently sized target DNA. Four different amounts of sample DNA were tested, from 0.1 to 3 fmol and the results are shown in **Figure 7**. For all four target DNA levels tested, the presence and amount of nonspecific sequences did not have a significant effect on hybridization for a mass ratio up to 300-fold in comparison to pSD5. This result suggests that, if applied to detecting genomic DNA, the assay would be able to achieve a similar level of sensitivity. If we assume the assay could reach 0.02 fmol in detecting *E. coli* genomic DNA, with a size of 4.6 Mbp, the limit of detection in mass would be about 0.5 μg, or $\approx 1 \times 10^7$ cells equivalent, which is close to that of microarray systems for detecting PCR amplicons.[45]

3.4. Multiplex Detection

As mentioned earlier, a prominent advantage of the QdotB-based assay is the ability for flexible multiplex screening. This is realized by using microbeads encoded differently with QDs and conjugated with different probes. Here, we conducted a 3-plex hybridization assay for the three genes of *Neomycin, Ampicillin*, and *Lac Z*. Microbeads doped with varying ratios of 500- and 600-nm QDs were employed, as shown in the scatter plot in **Figure 8**a as three distinct clusters. The design of plasmid digestion and probe sets for each gene followed the principles concluded from Section 3.2, that is, generating a target fragment of 35–50 bp while minimizing the structure of hairpin loops within the probe and target sequences. Meanwhile, cross hybridization between any of the target gene and the nonspecific probes was also minimized. The target and probe sequences are shown in Table 2.

The hybridization assay was conducted by mixing together all of the different capture-probe-conjugated QdotBs, reporter probes, along with the sample of digested plasmid DNA, with the same experimental procedures as for the single-plex assay. A series of different plasmid DNAs containing distinct combinations of the three genes were tested. As can be seen from the results shown in Figure 8b, the multiplex assay worked successfully. Positive and negative samples for any of the three genes can be distinguished unambiguously with no cross hybridization observed. The results were identical with independent single-plex assays. The lower signal for *Lac Z* as compared to the other two genes is rooted in the dependence of hybridization signal on the sequence/secondary structure of target and probes, as discussed in Section 3.2. Meanwhile, there was also an appreciable difference in the signal intensities especially for the gene of *Neo*, where the signal of pSD5 was almost five times stronger than that of pHTR3-B. This variation in hybridization yield should be attributed to matrix effects (interference from nontargeted fragments) for digested DNA samples, similar to that observed in Figure 5. This can be minimized in the future by including blocking reagents in the hybridization mixture. The results suggest that QdotBs are a flexible and reliable platform for multiplex genetic assay of crude and digested DNA samples.

small NANO MICRO

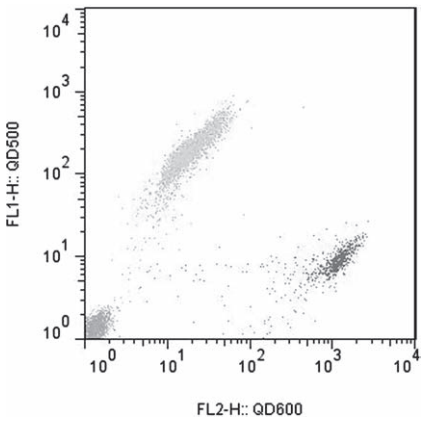

(a)

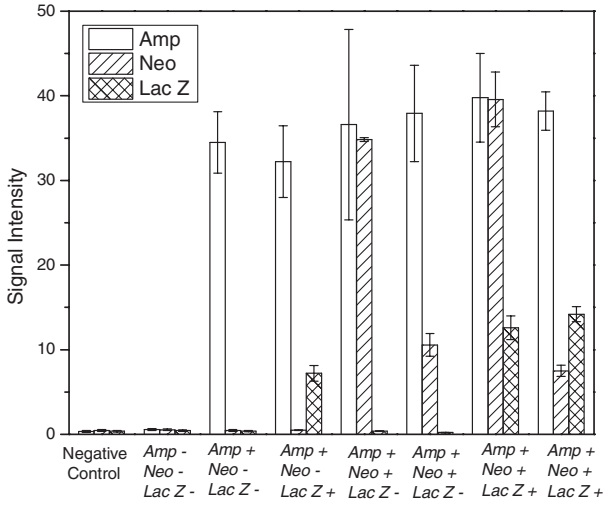

(b)

Figure 8. Simultaneous detection of the three genes of Amp, Neo, and Lac Z with three different QdotBs: a) optical mapping of the three QdotBs and b) assay results. The negative control contained no DNA. The model plasmids, from left to right, are pDONR211, pCX-ECFP, pGTlox4, plox511pNeo, pPGK-neo-FRT, pSD5, and pHTR3-B, respectively. The amount of sample DNA was 5 fmol for each assay.

4. Conclusion

We have examined a quantum-dot barcode (QdotB)-based multiplex hybridization assay for detecting DNA sequences cut using restriction endonucleases. Our results demonstrated that short probes (15–18 nt) and short DNA target (36 bp) produced optimal hybridization rate and efficiency. In spite of the crudeness of digested DNA sample, the optimized assay achieved a dynamic range of 3.5 logs and a limit of detection of 0.02 fmol. Matrix effects from noncomplementary DNA strands were observed under certain conditions and proved to be independent of the average size and amount of the noncomplementary sequences in the sample solution but more likely due to competition from certain cut sequences. In future, the use of blocking reagents in the hybridization mixture could reduce the matrix effects. This preliminary work on a digestion-based, non-PCR assay achieved satisfactory detection performance with simpler assay procedures than other techniques. Furthermore, QdotBs can be integrated in a microfluidic system to automate the assay process prior to read out in a flow-focusing channel.[18] These results take QdotBs one step closer towards their promise as a high-throughput, rapid, sensitive, and multiplex platform for genetic detection.

Acknowledgements

The authors thank Dr. Supratim Giri for preparing the QdotBs for the multiplex assay, David Li for preparing the quantum dots, Edward Sykes for his help with the hybridization experiment, and Tammy Reid for her help with preparation of plasmid DNA, and helpful discussions. W.C.W. and W.L.S. acknowledge NSERC (RGPIN 288231–09 and RGPIN 293170–04), CIHR (RMF-72557), CFI, and MRI for funding support.

[1] D. A. A. Vignali, *J. Immunol. Methods* **2000**, *243*, 243.
[2] T. D. Chung, H. C. Kim, *Electrophoresis* **2007**, *28*, 4511.
[3] M. Han, X. Gao, J. Z. Su, S. Nie, *Nat. Biotechnol.* **2001**, *19*, 631.
[4] A. Sukhanova, I. Nabiev, *Crit. Rev. Oncol. Hematol.* **2008**, *68*, 39.
[5] R. Wilson, A. R. Cossins, D. G. Spiller, *Angew. Chem.* **2006**, *118*, 6250; *Angew. Chem. Int. Ed.* **2006**, *45*, 6104.
[6] K. D. Bake, D. R. Walt, *Annu. Rev. Anal. Chem.* **2008**, *1*, 515.
[7] A. Sukhanova, A. S. Susha, A. Bek, S. Mayilo, A. L. Rogach, J. Feldmann, V. Oleinikov, B. Reveil, B. Donvito, J. H. M. Cohen, I. Nabiev, *Nano Lett.* **2007**, *7*, 2322.
[8] K. Y. Lien, C. J. Liu, P. L. Kuo, G. B. Lee, *Anal. Chem.* **2009**, *81*, 4502.
[9] A. C. Jahns, R. G. Haverkamp, B. H. A. Rehm, *Bioconjugate Chem.* **2008**, *19*, 2072.
[10] C. Wilhelm, *Phys. Rev. Lett.* **2008**, *101*, 028101.
[11] E. Sykova, P. Jendelova, *Prog. Brain Res.* **2007**, *161*, 367.
[12] X. Gao, S. Nie, *Proc. SPIE* **2004**, *5593*, 292.
[13] Y. Yang, Z. Wen, Y. Dong, M. Gao, *Small* **2006**, *2*, 898.
[14] M. Strömberg, T. Zardán Gómez De La Torre, J. Göransson, K. Gunnarsson, M. Nilsson, P. Svedlindh, M. Strømme, *Anal. Chem.* **2009**, *81*, 3398.
[15] S. Fournier-Bidoz, T. L. Jennings, J. M. Klostranec, W. Fung, A. Rhee, D. Li, W. C. W. Chan, *Angew. Chem.* **2008**, *120*, 5659; *Angew. Chem. Int. Ed.* **2008**, *47*, 5577.
[16] T. L. Jennings, K. S. Rahman, S. Fournier-Bidoz, W. C. W. Chan, *Anal. Chem.* **2008**, *80*, 2849.
[17] J. A. Lee, S. Mardyani, A. Hung, A. Rhee, J. Klostranec, Y. Mu, D. Li, W. C. W. Chan, *Adv. Mater.* **2007**, *19*, 3113.
[18] J. M. Klostranec, Q. Xiang, G. A. Farcas, J. A. Lee, A. Rhee, E. I. Lafferty, S. D. Perrault, K. C. Kain, W. C. W. Chan, *Nano Lett.* **2007**, *7*, 2812.
[19] H. Xu, M. Y. Sha, E. Y. Wong, J. Uphoff, Y. Xu, J. A. Treadway, A. Truong, E. O'Brien, S. Asquith, M. Stubbins, N. K. Spurr, E. H. Lai, W. Mahoney, *Nucleic Acids Res.* **2003**, *31*,e43.
[20] P. S. Eastman, W. Ruan, M. Doctolero, R. Nuttall, G. De Feo, J. S. Park, J. S. F. Chu, P. Cooke, J. W. Gray, S. Li, F. F. Chen, *Nano Lett.* **2006**, *6*, 1059.
[21] C. To, T. Epp, T. Reid, Q. Lan, M. Yu, C. Y. Li, M. Ohishi, P. Hant, N. Tsao, G. Casallo, J. Rossant, L. R. Osborne, W. L. Stanford, *Nucleic Acids Res.* **2004**, *32*, D557.
[22] A. K. Hadjantonakis, S. MacMaster, A. Nagy, *BMC Biotechnol.* **2002**, *2*, 11.

[23] B. Sauer, M. Whealy, A. Robbins, L. Enquist, *Proc. Natl. Acad. Sci. USA* **1987**, *84*, 9108.
[24] W. L. Stanford, unpublished.
[25] P. H. Rogers, E. Michel, C. A. Bauer, S. Vanderet, D. Hansen, B. K. Roberts, A. Calvez, J. B. Crews, K. O. Lau, A. Wood, D. J. Pine, P. V. Schwartz, *Langmuir* **2005**, *21*, 5562.
[26] A. W. Peterson, R. J. Heaton, R. M. Georgiadis, *Nucleic Acids Res.* **2001**, *29*, 5163.
[27] T. M. Herne, M. J. Tarlov, *J. Am. Chem. Soc.* **1997**, *119*, 8916.
[28] A. B. Steel, R. L. Levicky, T. M. Herne, M. J. Tarlov, *Biophys. J.* **2000**, *79*, 975.
[29] B. Tinland, A. Pluen, J. Sturm, G. Weill, *Macromolecules* **1997**, *30*, 5763.
[30] N. Zammatteo, I. Alexandre, I. Ernest, L. Le, F. Brancart, J. Remacle, *Anal. Biochem.* **1997**, *253*, 180.
[31] M. Ranki, A. Palva, M. Virtanen, *Gene* **1983**, *21*, 77.
[32] E. Southern, K. Mir, M. Shchepinov, *Nat. Genet.* **1999**, *21*, 5.
[33] W. T. Liu, H. Guo, J. H. Wu, *Appl. Environ. Microbiol.* **2007**, *73*, 73.
[34] J. G. Wetmur, N. Davidson, *J. Mol. Biol.* **1968**, *31*, 349.
[35] T. R. Hughes, M. Mao, A. R. Jones, J. Burchard, M. J. Marton, K. W. Shannon, S. M. Lefkowitz, M. Ziman, J. M. Schelter, M. R. Meyer, S. Kobayashi, C. Davis, H. Dai, Y. D. He, S. B. Stephaniants, G. Cavet, W. L. Walker, A. West, E. Coffey, D. D. Shoemaker, R. Stoughton, A. P. Blanchard, S. H. Friend, P. S. Linsley, *Nat. Biotechnol.* **2001**, *19*, 342.
[36] F. C. Tenover, *Clin. Microbiol. Rev.* **1988**, *1*, 82.
[37] V. J. Denef, J. Park, J. L. M. Rodrigues, T. V. Tsoi, S. A. Hashsham, J. M. Tiedje, *Environ. Microbiol.* **2003**, *5*, 933.
[38] S. A. M. Martins, D. M. F. Prazeres, L. P. Fonseca, G. A. Monteiro, *Anal. Bioanal. Chem.* **2009**, *394*, 1711.
[39] S. M. Tiquia, L. Wu, S. C. Chong, S. Passovets, D. Xu, Y. Xu, J. Zhou, *BioTechniques* **2004**, *36*, 664.
[40] A. Relógio, C. Schwager, A. Richter, W. Ansorge, J. Valcárcel, *Nucleic Acids Res.* **2002**, *30*.
[41] Y. Gao, L. K. Wolf, R. M. Georgiadis, *Nucleic Acids Res.* **2006**, *34*, 3370.
[42] H. Hakala, P. Heinonen, A. Iitiä, H. Lönnberg, *Bioconjugate Chem.* **1997**, *8*, 378.
[43] K. Kerman, Y. Matsubara, Y. Morita, Y. Takamura, E. Tamiya, *Sci. Technol. Adv. Mater.* **2004**, *5*, 351.
[44] K. A. Edwards, A. J. Baeumner, *Anal. Chem.* **2006**, *78*, 1958.
[45] J. Small, D. R. Call, F. J. Brockman, T. M. Straub, D. P. Chandler, *Appl. Environ. Microbiol.* **2001**, *67*, 4708.

Received: May 27, 2010
Published online: November 25, 2010

